Journal of Molecular Spectroscopy 305 (2014) 10–16

Contents lists available at ScienceDirect

Journal of Molecular Spectroscopy

journal homepage: www.elsevier.com/locate/jms

Quantitative mid-infrared spectra of allene and propyne from room to high temperatures

Et. Es-sebbar [a], A. Jolly [b], Y. Benilan [b], A. Farooq [a,*]

[a] Chemical Kinetics and Laser Sensors Laboratory, Clean Combustion Research Center, Division of Physical Sciences and Engineering, King Abdullah University of Science and Technology (KAUST), Thuwal 23955-6900, Saudi Arabia

[b] Laboratoire Interuniversitaire des Systèmes Atmosphériques (LISA), UMR 7583 du CNRS, Universités Paris-Est Créteil et Paris Diderot, Institut Pierre Simon Laplace, 61 Avenue du Général de Gaulle, 94010 Créteil, France

ARTICLE INFO

Article history:
Received 31 May 2014
In revised form 29 August 2014
Available online 30 September 2014

Keywords:
Allene
Propyne
Infrared absorption cross-section
Integrated intensities
FTIR

ABSTRACT

Allene (a-C_3H_4; CH_2CCH_2) and propyne (p-C_3H_4; CH_3C_2H) have attracted much interest because of their relevance to the photochemistry in astrophysical environments as well as in combustion processes. Both allene and propyne have strong absorption in the infrared region. In the present work, infrared spectra of a-C_3H_4 and p-C_3H_4 are measured in the gas phase at temperatures ranging from 296 to 510 K. The spectra are measured over the 580–3400 cm^{-1} spectral region at resolutions of 0.08 and 0.25 cm^{-1} using Fourier Transform Infrared spectroscopy. Absolute integrated intensities of the main infrared bands are determined at room temperature and compared with values derived from literature for both molecules. Integrated band intensities are also determined as a function of temperature in various spectral regions.

1. Introduction

Allene (a-C_3H_4; CH_2CCH) and propyne (p-C_3H_4; CH_3C_2H) have attracted much interest for a long time because of their relevance to the photochemistry in planetary environments [1–8]. More recently, infrared (IR) spectra at high temperatures have gained a lot of interest because of the warm atmospheres of exoplanets, known as "Hot Jupiters", which are now being extensively studied [9,10]. Furthermore, a-C_3H_4 and p-C_3H_4 represent key intermediates in combustion processes [11–16]. They are ubiquitous and play a crucial role in the formation of propargyl radical, a key intermediate in the production of aromatic compounds and soot particles [11–13].

Both allene and propyne absorb strongly in the IR domain (see Linnett et al. [17]; Rasmussen et al. [18]; Mills et al. [19]; Stone [20]; Koga et al. [21]; Kondo and Koga [22]; Maki and Pine [23]) thus providing possibilities for sensitive detection in extraterrestrial environments for both molecules. Allene may be present in Titan and in the atmosphere of giants planets including Jupiter [24] and Saturn [8,25]. However, only propyne has so far been detected in the atmosphere of Titan [1,3,26,27]. As pointed out by Teanby et al. [7], the determined abundance of propyne in Titan's atmosphere is questionable due to the uncertainties in the laboratory measurements. In addition, the absence of allene is difficult to explain by photochemical models since both isomers are expected to transform into each other, undergoing similar processes. It has been proposed that perhaps complete isomerization of a-C_3H_4 into p-C_3H_4 occurs.

In the mid-IR spectral domain, the strongest fundamental bands of allene are observed near 841 (ν_{10}), 999 (ν_9) and 1957 cm^{-1} (ν_6). The strongest transitions of propyne in the mid-IR are observed near 633 (ν_9), 1452 (ν_7) and 3334 cm^{-1} (ν_1). Over the last few decades, the spectroscopic characterization of a-C_3H_4 and p-C_3H_4 in the laboratory has been the topic of many studies using various spectroscopic diagnostics. Fourier Transform Infrared (FTIR) spectroscopy studies have been used to analyze the IR spectra and determine vibrational assignments and molecular structure (see Refs. [28–30]). High-resolution tunable diode laser spectroscopy has been used to determine line intensities and collisional broadening parameters [31–34] as well as rotational and molecular constants [35–38].

This paper is part of our studies on gas-phase spectroscopy of molecules relevant to the photochemistry in planetary atmospheres, warm exoplanetary atmospheres and combustion processes. To enable the study of allene and propyne in such environments, and in order to provide extensive information about the constituents of planetary atmospheres as well as their excitation processes, high quality IR spectra are needed. In combustion processes, IR data will be used for the development of high-tem-

* Corresponding author.
E-mail address: aamir.farooq@kaust.edu.sa (A. Farooq).

http://dx.doi.org/10.1016/j.jms.2014.09.004
0022-2852/

perature quantitative diagnostics to study the decomposition of allene and propyne using shock tube and rapid compression machines. In the present study, we report the IR spectra of a-C_3H_4 and p-C_3H_4 as a function of temperature (296–510 K). Section 2 presents our experimental setup used to measure absorption spectra and in Section 3 we describe briefly the procedure used to retrieve cross-sections and integrated intensities. IR spectra and band assignments are presented in Section 4 and finally, we present the integrated intensities and the influence of high temperatures.

2. Experimental method

IR spectra were measured between 580 and 3400 cm^{-1} using a Fourier Transform Infrared (FTIR) spectrometer (Bruker Vertex 80V). The experimental setup was described previously for the investigation of 1-butene and propylene (see Es-sebbar et al. [39,40]) and only a brief description is given here. A KBr beamsplitter, a Globar mid-IR source and a DLaTGS detector were used to record the spectra. Based on the maximum interferometer mirror displacement, spectral resolution up to 0.06 cm^{-1} can be reached. Here, entrance aperture diameters of 2 and 2.5 mm and a collimating mirror of 100 mm focal length were used. These settings results in spectral resolution of 0.08 and 0.25 cm^{-1}. The interferograms were corrected with the Mertz phase function and the boxcar apodized interferograms were zero-filled to produce the final spectrum. The modulated IR light was transmitted through an optical cell, made of stainless steel and equipped with KBr windows. The cell placed inside the chamber of the FTIR instrument, has an optical path length of 10 cm. To record spectra at high temperatures, the absorption cell was heated using a heating jacket connected to a controller system. The temperature was measured continuously with five type-K (Omega) thermocouples along the length of the absorption cell with an uncertainty less than 0.5%.

Ultra-pure (99.999%) a-C_3H_4 and p-C_3H_4, purchased from Abdullah Hashim Industrial Gases & Equipment Co. Ltd., were used for IR studies. Spectra were recorded with pure samples and also with a mixture of 4% a-C_3H_4 in N_2. Measurements were made at various temperatures ranging from 296 to 510 K. At each temperature, series of spectra were recorded between 580 and 3400 cm^{-1} for various pressures. The pressure was monitored using three Baratron capacitance gauges (20, 100, and 1000 Torr full-scale ranges). Before and after each measurement, 120 co-added scans were recorded with the cell evacuated to take into account any drift in the background intensity. The absorption cell was evacuated to about 1×10^{-4} Torr using a turbo-molecular pump (Turbo-v 81-M Varian) backed by a rotary mechanical pump (Varian DS-102). For the room-temperature (296 K) measurements, the entire FTIR compartment was evacuated to less than 0.1 mbar to avoid absorption by CO_2 and H_2O. For high-temperature measurements, N_2 gas was used to purge the FTIR spectrometer. To calibrate the FTIR wavenumber scale and to assign the observed features with corresponding line positions, spectra of CO and CH_4 gases were recorded and compared with the corresponding lines in the HITRAN database.

3. Data analysis

The absorbance, A_ν, can be written using the Beer–Lambert law:

$$A_\nu = \ln (I_0/I)_\nu = \varepsilon_\nu(lp) \quad (1)$$

where I_0 is the incident intensity recorded with the empty cell (background), I is the transmitted intensity measured with a-C_3H_4 or p-C_3H_4 samples, ε_ν is the absorption coefficient at wavenumber ν in cm^{-1} atm^{-1}, l is the optical path length in cm; and p is the gas pressure in atm.

The absorption coefficient ε_ν can be converted to cross-section values (cm^2/molecule) using:

$$\sigma_\nu = (\varepsilon_\nu/N)(T\ (\mathrm{K})/273.15) \quad (2)$$

where $N = 2.68676 \times 10^{19}/cm^3$ is the Loschmidt number at standard values of temperature and pressure (273.15 K/1013.25 mbar).

In order to determine the integrated band intensity (S_ν), given in cm^{-2} atm^{-1}, the integrated absorbance ($\int A_\nu\ d\nu$) is first calculated as a function of gas pressure for different a-C_3H_4 and p-C_3H_4 bands. Then integrated absorbance ($\int A_\nu\ d\nu$) is plotted as a function of the product of the optical path length and the partial pressure of the sample (lp):

$$\int A_\nu\ d\nu = (lp)\int \varepsilon_\nu\ d\nu = (lp)S_\nu \quad (3)$$

The linear dependence of the integrated absorbance with lp is systematically verified and the absolute integrated intensity (S_ν) is deduced from the slope of the linear fit. These integrated intensity values are compared with quantitative results taken from the PNNL database [41]. Absorbance spectra taken from PNNL database were first converted to cross-section values by combining Eqs. (1) and

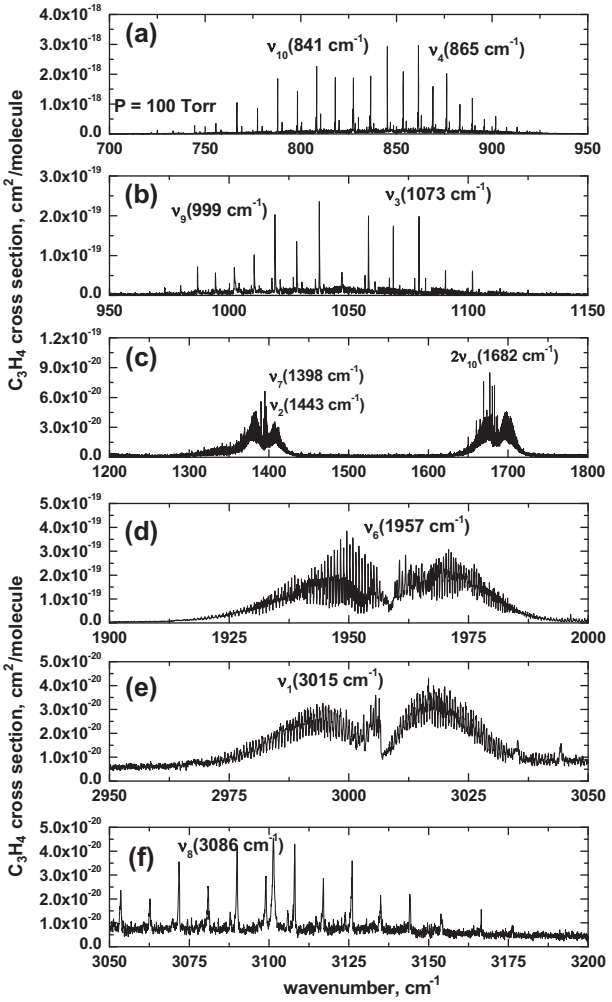

Fig. 1. Allene absorption cross-sections between 700 and 3200 cm^{-1} at 296 K. Spectra are recorded for 4% a-C_3H_4/N_2 mixture and the total pressure is 100 Torr. The main features are identified and summarized in Table 1. Spectra between 700 and 1150 are recorded at spectral resolution of 0.08 cm^{-1}. Spectra in the 1200–3200 cm^{-1} range are recorded at 0.25 cm^{-1} resolution.

Table 1
Vibrational modes of allene. The peak positions correspond to the maximum value of the cross-sections (w: weak, m: medium, s: strong, vs: very strong).

Band	Peak position (cm^{-1})	Vibrational assignment
ν_1 (a_1)	3015 (not observed)	CH_2 stretching
ν_2 (a_1)	1443 (not observed)	CH_2 scis
ν_3 (a_1)	1073 (not observed)	CC stretching
ν_4 (b_1)	865 (not observed)	CH_2 twist
ν_5 (b_2)	3015 (w)	CH_2 stretching
ν_6 (b_2)	1957 (m)	CC stretching
ν_7 (b_2)	1398 (m)	CH_2 scis
ν_8 (e)	3086 (m)	CH_2 stretching
ν_9 (e)	999 (s)	CH_2 rock
ν_{10} (e)	841 (vs)	CH_2 wag
ν_{11} (e)	352 (out of range)	CCC bend

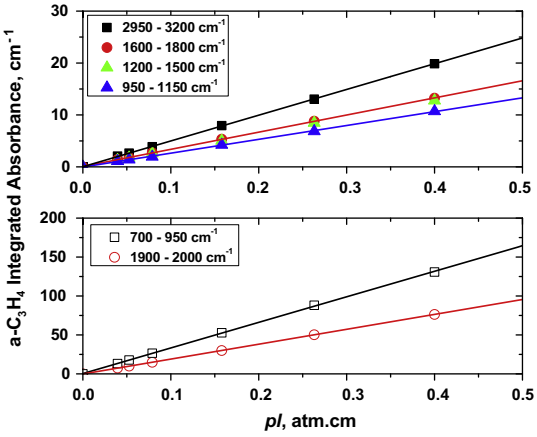

Fig. 2. Integrated absorbance (base-e) of allene (a-C_3H_4) as a function of the product of its partial pressure and optical path length for various wavenumber regions. Spectra are recorded in a mixture of 4% a-C_3H_4/N_2 for a total pressure up to 1 atm.

(2) for an optical path length of 100 cm and a pressure of 1.013×10^{-3} mbar. Cross-sections were integrated over the studied spectral regions to compare with our integrated band intensities.

Uncertainties in cross-section measurements result primarily from uncertainties in the measured absorbance, the optical path length, the gas pressure and the gas temperature. The uncertainty on the optical path length is less than 0.5% arising from the expansion of the cell as the temperature increases. The measured pressure has an uncertainty of less than 2%, which results from the uncertainty in the Baratron measurement and the pressure variation due to the adsorption of the sample on the cell walls. The uncertainty in temperature is about 0.5%, arising from the statistical error of the readings given by the five thermocouples and from the temperature gradient over the length of the optical cell. Due to relatively small absorption over 2800–3400 cm^{-1} spectral region, the error on the absorbance can be higher. This weakness was compensated by performing measurements at higher pressures. The uncertainty due to the drift of the intensity signal was evaluated by measuring the background before and after sample measurements. The combination of all error sources yields an overall uncertainty of about ±3% in the measured absorption cross-sections in the 580–2800 cm^{-1} range and ±5% uncertainty in the relatively higher wave number range of 2800–3400 cm^{-1}.

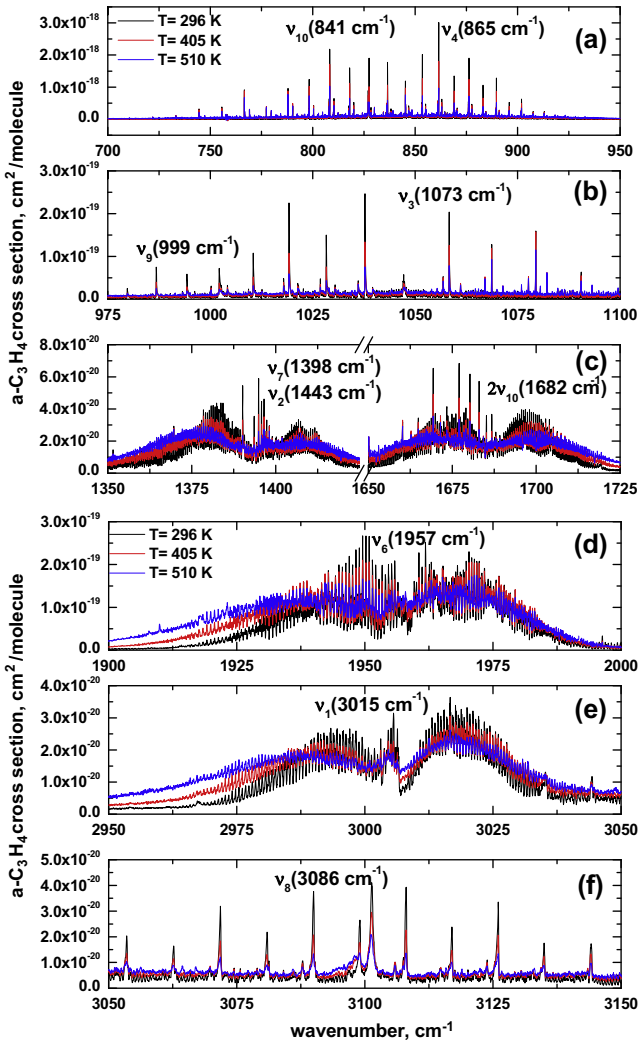

Fig. 3. IR cross-section for a-C_3H_4 at 296, 405 and 510 K. Spectra are recorded with a pure sample at low pressures: (5 Torr for 700–950 cm^{-1} range; 50 Torr for 1350–1725 cm^{-1} and 20 Torr for all other spectral domains). The resolution is 0.08 cm^{-1} in the 700–1150 cm^{-1} range and 0.25 cm^{-1} between 1200 and 3150 cm^{-1}.

Table 2
Integrated band intensities at 296 K, obtained using a 4% allene/N_2 mixture and spectral resolutions of 0.08 and 0.25 cm^{-1} compared to PNNL data of Sharpe et al. [41] (resolution: 0.112 cm^{-1}) and Koga et al. [21] (resolution: 1 cm^{-1}). The percentage difference between the present data and the literature is given by: $\% \delta = 100 \times (S_{this\ work} - S_{literature})/S_{literature}$.

Vibrational modes	Wavenumber range (cm^{-1})	S_{band} (296 K) cm^{-2} atm^{-1} This work	$S_{band} \times 10^{-18}$ cm/molecule This work	$S_{band} \times 10^{-18}$ cm/molecule Sharpe et al. [41]	$S_{band} \times 10^{-18}$ cm/molecule Koga et al. [21]	% δ with [41]	% δ with [21]
$\nu_5 + \nu_8$	2950–3200	49.56 ± 2.5	2.00 ± 0.1	1.68 ± 0.03	2.06	+19.0	−2.9
$\nu_6 + 2\nu_9$	1900–2000	212.8 ± 6.0	8.58 ± 0.24	8.22 ± 0.22	8.11	+4.4	+5.8
$2\nu_{10}$	1600–1800	33.4 ± 1.2	1.35 ± 0.05	1.37 ± 0.05	–	−1.5	–
ν_7	1200–1500	33.6 ± 1.5	1.35 ± 0.06	1.41 ± 0.03	1.16	−4.2	+16.4
ν_9	950–1150	36.2 ± 1.3	1.46 ± 0.05	1.42 ± 0.12	1.46	+2.8	0
ν_{10}	700–950	375.9 ± 6.6	15.2 ± 0.3	15.51 ± 1.71	15.1	−2.0	+0.7

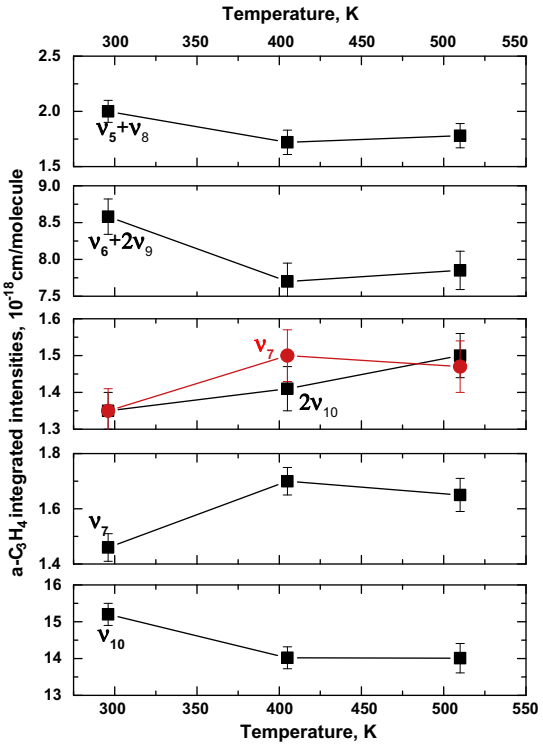

Fig. 4. Integrated band intensities as a function of temperature for various bands of a-C_3H_4. Temperature is changed from 296 to 510 K.

4. Results and discussion

4.1. Allene absorption spectra

4.1.1. Room-temperature spectra and vibrational assignments

Fig. 1 shows the IR cross-sections of allene at 296 K measured at spectral resolutions of 0.08 and 0.25 cm^{-1}. For clarity, the recorded spectrum is divided into different regions. To avoid saturation of the absorption bands, spectra were recorded in a mixture of 4% a-C_3H_4/N_2. Allene has eleven vibrational modes (see Table 1) but only seven modes are infrared active. Except for the low energy ν_{11} mode centered at 352 cm^{-1} which is not in the range of our instrument, all other active modes are observed in this study. Between 700 and 950 cm^{-1} (Fig. 1a) we observe the strongest absorption band due to the ν_{10} mode (841 cm^{-1}). We also identify ν_9 at 999 cm^{-1} (Fig. 1b) followed by ν_7 at 1398 cm^{-1} and a strong overtone band at 1682 cm^{-1} ($2\nu_{10}$) (Fig. 1c). In the spectral region between 1900 and 2000 cm^{-1} (Fig. 1d), the ν_6 mode is observed (1957 cm^{-1}) together with a small contribution of an overtone band which is $2\nu_9$. The CH_2 symmetric stretching mode ν_5 (3015 cm^{-1}) (Fig. 1e) is also observed in our spectra together with the asymmetric CH_2 stretching mode ν_8 at 3086 cm^{-1} (Fig. 1f).

4.1.2. Room-temperature integrated band intensities

Absorption measurements are performed for various pressures to determine the integrated intensities for all bands of allene described above. Integrated absorbances (base-e) are plotted as a function of the product of the partial pressure of a-C_3H_4 the and optical path length (*pl*) (Fig. 2). Spectra are recorded in a mixture of 4% a-C_3H_4/N_2 for a maximum total pressure of 1 atm. As can be seen in Fig. 2, the resulting integrated absorbances show a clear linear dependence. For all selected spectral regions, high correlation coefficients of ~0.99 are obtained. The integrated intensities for various features are calculated from the slopes of the linear fits. Retrieved values and corresponding uncertainties are listed in Table 2. For comparison, values derived from the PNNL database [41] and Koga et al. [21] are also shown. Our results agree very well with the PNNL data, within the estimated uncertainties, except for the integrated intensity between 2950 and 3200 cm^{-1} where our result is higher by 19%. Moreover, an excellent agreement is observed with the values from Koga et al. [21], except for the 1200–1500 cm^{-1} region where our measurements are higher by about 16%.

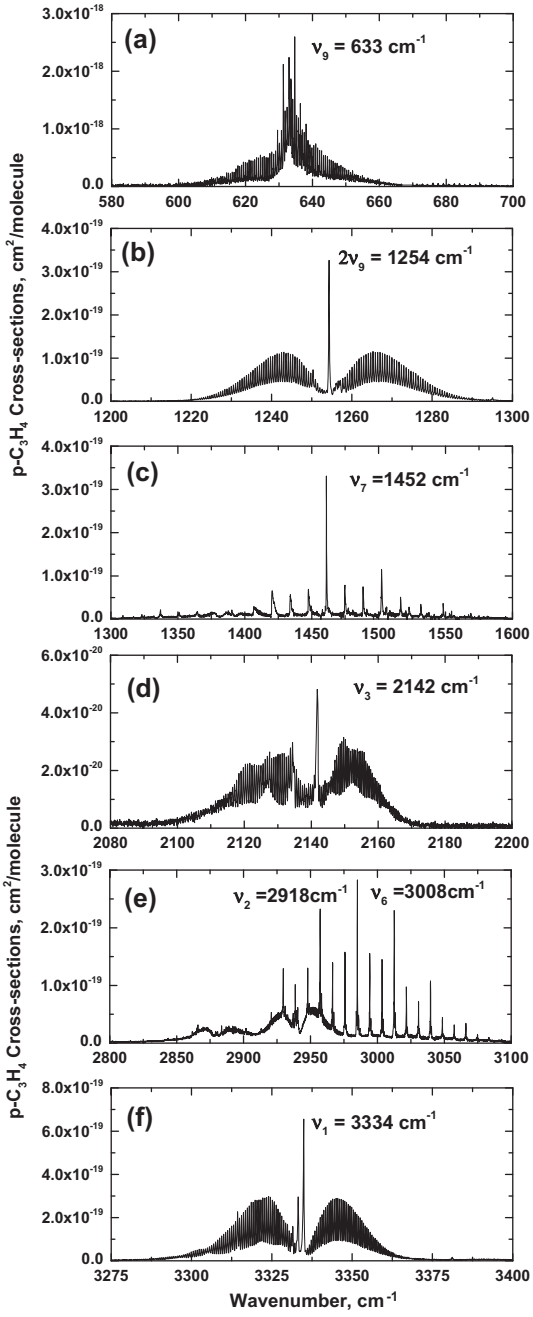

Fig. 5. Propyne absorption cross-section measured between 580 and 3400 cm^{-1} at 296 K. Spectra are recorded with 4% propyne/N_2 mixture and a total pressure between 150 and 400 Torr (see text). The main features are identified and summarized in Table 3. Spectra in the 700–1300 cm^{-1} are recorded at a resolution of 0.08 cm^{-1} and spectra in the 1300–3400 cm^{-1} are recorded at 0.25 cm^{-1} resolution.

4.1.3. Variation of absorption spectra with temperature

The effect of the temperature on the IR spectra of allene is studied by recording spectra at 296, 405 and 510 K. The variation of

Table 3
Vibrational modes of propyne. The peak positions correspond to the maximum value of the cross-sections (w: weak, m: medium, s: strong, vs: very strong).

Band	Peak position (cm^{-1})	Vibrational assignment
ν_1 (a_1)	3334 (vs)	CH stretching
ν_2 (a_1)	2918 (s)	CH_3 stretching
ν_3 (a_1)	2142 (m)	CC stretching
ν_4 (a_1)	1382 (not observed)	CH_3 deformation
ν_5 (a_1)	931 (not observed)	CC stretching
ν_6 (e)	3008 (s)	CH_3 stretching
ν_7 (e)	1452 (s)	CH_3 deformation
ν_8 (e)	1053 (not observed)	CH_3 rock
ν_9 (e)	633 (vs)	CH bend
ν_{10} (e)	327 (out of range)	CCC bend

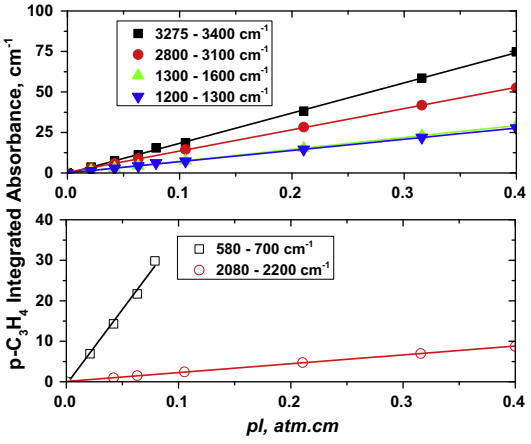

Fig. 6. Integrated absorbance (base-e) of propyne as a function of the product of its partial pressure and optical path length for various wavenumber regions. Spectra are recorded with a mixture of 4% p-C_3H_4/N_2 for a maximum total pressure of 150 Torr in the case of 580–700 cm^{-1} region and 1 atm for all other spectral regions.

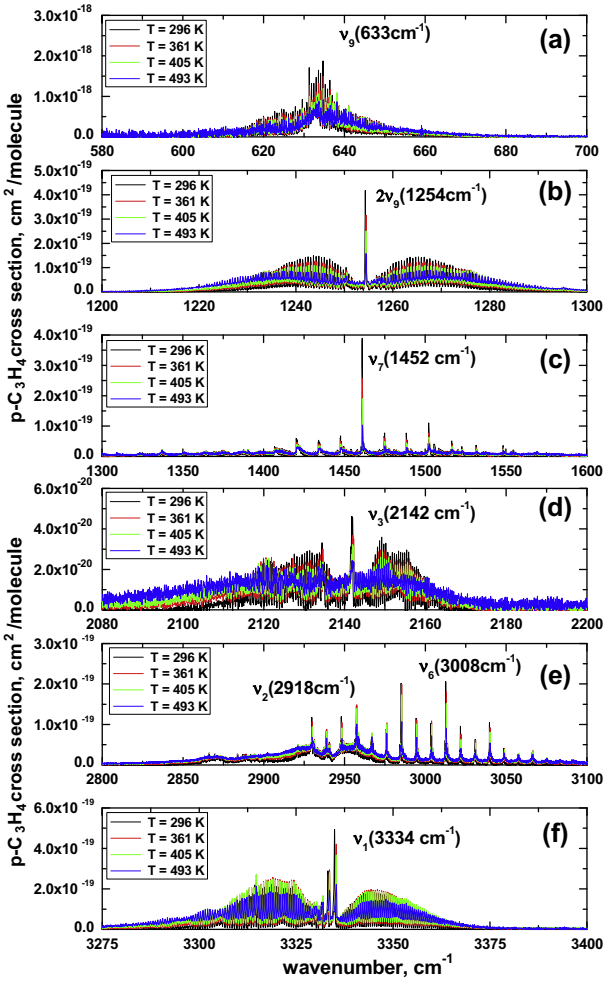

Fig. 7. IR cross-section measurements of p-C_3H_4 at 296, 361, 405 and 493 K. Spectra are recorded with a pure sample at low pressures: (2 Torr in 580–700 cm^{-1} range and 10 Torr for all other spectral domains). The resolution is 0.08 cm^{-1} in the 700–1300 cm^{-1} range and 0.25 cm^{-1} between 1300 and 3400 cm^{-1}.

absorption cross-sections with temperature is studied using pure allene to achieve high signal-to-noise-ratio. We compared cross-section data obtained in pure sample with allene/N_2 mixture; reliable spectra were obtained and the instrument function did not affect pure sample measurements. Fig. 3 shows the absorption cross-sections for all observed bands for all three temperatures. When temperature increases, we mainly observe a significant decrease of the sharp absorption peaks and an extension of the absorption to a wider range. A similar temperature dependence of IR cross-sections was previously observed and discussed for 1-butene [39] and propylene [40]. This effect is mainly due to changes in the vibrational and rotational population distribution.

Integrated band intensities at 405 and 510 K are determined similarly to the room-temperature band intensities. The retrieved intensities are shown in Fig. 4. Changing the temperature from 296 to 510 K leads to small variations in the integrated intensities with maximum differences reaching 13%. These variations are higher than our expected measurement uncertainties, however, it is difficult to determine if the integrated intensity is temperature dependent or not since we did not observe a clear trend. The integrated intensity of each band system should generally be independent of temperature for isolated features comprising primarily fundamental vibrational bands [41–44]. However, as pointed out by earlier studies [45–47], anharmonicities, overlapping features from neighboring bands as well as contributions from overtones and combination/difference bands can be responsible for small variations of the integrated intensities with temperature.

Table 4
Integrated band intensities at 296 K, obtained using a 4% propyne/N_2 mixture and spectral resolution of 0.08 and 0.25 cm^{-1} compared to PNNL of Sharpe et al. [41] (resolution: 0.112 cm^{-1}) and Kondo and Koga [22] (resolution: 0.1 cm^{-1}). Here, $\% \delta = 100 \times (S_{thiswork} - S_{literature})/S_{literature}$.

Vibrational modes	Wavenumber range (cm^{-1})	S_{band} (cm^{-2} atm^{-1}) This work	$S_{band} \times 10^{-18}$ cm/molecule This work	$S_{band} \times 10^{-18}$ cm/molecule Sharpe et al. [41]	$S_{band} \times 10^{-18}$ cm/molecule Kondo et Koga [22]	% δ with [41]	% δ with [22]
ν_1	3275–3400	186.58 ± 7.55	7.53 ± 0.30	7.45 ± 0.65	7.5 ± 0.5	+1.1	+0.4
$\nu_2 + \nu_6$	2800–3100	131.25 ± 6.52	5.30 ± 0.26	5.12 ± 0.32	5.4 ± 0.6	+3.5	−1.8
ν_3	2080–2200	21.87 ± 0.63	0.88 ± 0.02	0.82 ± 0.04	0.88 ± 0.05	+7.3	0
ν_7	1300–1600	73.68 ± 1.20	2.97 ± 0.05	2.98 ± 0.27	2.97 ± 0.3	−0.3	0
$2\nu_9$	1200–1300	69.20 ± 1.20	2.79 ± 0.05	2.79 ± 0.26	–	0	–
ν_9	580–700	371.12 ± 8.0	14.96 ± 0.32	14.75 ± 1.52	14.50 ± 0.8	+1.4	+3.2

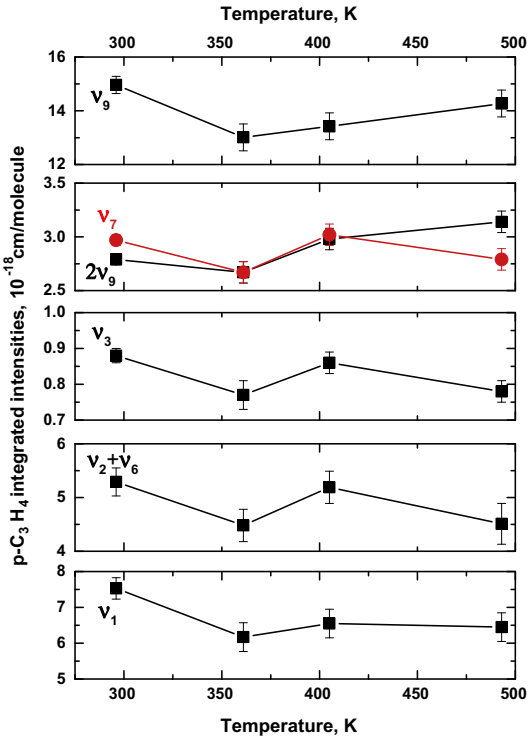

Fig. 8. Integrated band intensities as a function of temperature for various bands of p-C_3H_4.

4.2. Propyne absorption spectra

4.2.1. Room-temperature spectra and vibrational assignments

IR spectra of propyne at 296 K are shown in Fig. 5(a–f) over the 580–3400 cm^{-1} region. All measurements are recorded using a 4% p-C_3H_4/N_2 mixture. Spectra are recorded at a total pressure of 400 Torr to get data with high signal-to-noise ratio, except for the 580–700 cm^{-1} spectral region where spectra are recorded at 150 Torr to avoid signal saturation. The mid-IR spectra of propyne reveal several prominent features. The fundamental vibrational modes of propyne are listed in Table 3 along with the characteristic frequencies. In the low wavenumber range, 580–700 cm^{-1} (Fig. 5a), a very strong absorption band is observed near 633 cm^{-1} corresponding to the ν_9 C–H bending mode. The region from 1200 to 1300 cm^{-1} is dominated by the $2\nu_9$ overtone band (Fig. 5b) followed, between 1300 and 1600 cm^{-1} (Fig. 5c) by a feature belonging to the CH_3 deformation mode ν_7 peaking near 1452 cm^{-1}. In the 2080–2200 cm^{-1} region (Fig. 5d), an absorption band is observed near 2142 cm^{-1} which is assigned to the ν_3 C–C stretching mode. Two overlapping features appear in the 2800–3100 cm^{-1} domain corresponding to ν_2 (2918 cm^{-1}) and ν_6 (3008 cm^{-1}) (Fig. 5e). In the 3275–3400 cm^{-1} range (Fig. 5f), the ν_1 (3334 cm^{-1}) CH stretching mode can be observed. All vibrational modes of propyne are active but the modes ν_4, ν_5, ν_8 are too weak to be measured in this work (see Kondo and Koga [22] for estimated intensities). Propyne also possesses a strong mode at 327 cm^{-1} which is out of the range of our experimental setup.

4.2.2. Room-temperature integrated band intensities

As in the case of allene, the band intensities of propyne are determined from the linear fit of the integrated absorbance versus the product (*pl*). The spectra of p-C_3H_4 have been divided into six spectral regions for the determination of integrated intensities. Fig. 6 shows the integrated absorbance versus *pl* for the considered six spectral regions. Spectra are recorded in a mixture of 4% p-C_3H_4/N_2 for a total pressure up to 150 Torr in the case of 580–700 cm^{-1} region to avoid any saturation and up to 1 atm for all other spectral regions. A linear dependence has been observed with a high correlation factor for all regions. Since the 2800–3100 cm^{-1} region contains two strongly overlapping bands (ν_2 and ν_6), a single integration has been carried out to cover the two features. By using Eq. (3), integrated intensities are derived and the resulting values and corresponding uncertainties are listed in Table 4. The estimated experimental uncertainties are better than 5%. For comparison, Table 4 also includes the derived integrated intensities from the PNNL database [41] and the measured band intensities by Kondo and Koga [22]. The overall agreement is very good since the largest difference is only 7.3% for the weak ν_3 band.

4.2.3. Variation of absorption spectra with temperature

Fig. 7 shows the IR spectra of propyne measured at 296, 361, 405 and 493 K for all six spectral regions. As expected, the temperature affects the shape of all the absorption bands. With increasing temperature, the intensities of the *Q* branches decrease while the *P* and *R* branches get wider and have their maxima moving away from the band center.

Integrated intensities for propyne are also determined for all four temperatures and all six absorption regions. The results are shown in Fig. 8. The integrated band intensities do not seem to be constant over the investigated temperature range as the observed variations are larger than our expected uncertainties. The largest difference is observed mainly for the ν_1 band where the integrated intensity decreases by about 18% when the temperature increases from 296 to 493 K (see Fig. 8). As observed for allene, such variations may point towards real variation of the integrated intensity with temperature due to the presence of overtone and combination bands. However, we do not observe a clear trend for the change of integrated intensities with temperature which makes it difficult to make a conclusive argument if the integrated intensities indeed exhibit some temperature dependence or not. There is little work in the literature that addresses temperature dependence of integrated intensities and further investigations are needed to ascertain this seemingly anomalous behavior.

5. Conclusion

The integrated intensities of allene and propyne measured in this work at room temperature are in very good agreement with previously published results. For both molecules, we observe variations of the integrated intensities with temperature with maximum variation being about 20%. Such variations are probably real since they are larger than our expected uncertainties and comparable with results from similar studies on other molecules. Measured spectra of allene and propyne are provided as Supplementary Material.

Acknowledgments

Research reported in this publication was supported by the King Abdullah University of Science and Technology (KAUST). The SIPAT program is funded in part by the Programme National de Planétologie of the Institut National des Sciences de l'Univers.

References

[1] A. Coustenis, B. Bézard, D. Gautier, Icarus 80 (1989) 54–76.
[2] B. Bézard, A. Coustenis, C.P. McKay, Icarus 113 (1995) 267–276.
[3] T. de Graauw, H. Feuchtgruber, B. Bézard, P. Drossart, T. Encrenaz, D.A. Beintema, J. Griffin, A. Heras, M.F. Kessler, K. Leech, E. Lellouch, A. Morris, P.R. Roelfsema, M. Roos-Serote, A. Salama, B. Vandenbussche, E.A. Valentijn, G.R. Davis, D.A. Naylor, Astron. Astrophys. 321 (1997) L13–L16.

[4] B. Bézard, P. Drossart, T. Encrenaz, H. Feuchtbruber, Icarus 155 (2001) 492–500.
[5] A. Coustenis, A. Salama, B. Schulz, S. Ott, E. Lellouch, Th. Encrenaz, D. Gautier, H. Feuchtgruber, Icarus 161 (2003) 383–403.
[6] S. Vinatier, B. Bézard, Th. Fouchet, N.A. Teanby, R. de Kok, P.G.J. Irwin, B.J. Conrath, C.A. Nixon, P.N. Romani, F.M. Flasar, A. Coustenis, Icarus 188 (2007) 120–138.
[7] N.A. Teanby, P.G.J. Irwin, R. de Kok, A. Jolly, B. Bézard, C.A. Nixon, S.B. Calcutt, Icarus 202 (2009) 620–631.
[8] S. Guerlet, Th. Fouchet, B. Bézard, J.I. Moses, L.N. Fletcher, A.A. Simon-Miller, F.M. Flasar, Icarus 209 (2010) 682–695.
[9] J. Tennyson, S.N. Yurchenko, Mon. Not. R. Astron. Soc. 425 (2012) 21–33.
[10] J. Tennyson, C. Hill, S.N. Yurchenko, AIP Conf. Proc. 1545 (2013) 186.
[11] M. Frenklach, S. Taki, M.B. Durgaprasad, R.A. Matula, Combust. Flame 54 (1983) 81–101.
[12] M. Frenklach, T. Yuan, M.K. Ramachandra, Energy Fuels 2 (1988) 462–480.
[13] M.J. Castaldi, A.M. Vincitore, S.M. Senkan, Combust. Sci. Technol. 107 (1995) 1–19.
[14] H. Curran, J.M. Simmie, Symp. (Int.) Combust. 26 (1996) 613–620.
[15] R. Fournet, J.C. Bauge, F. Battin-Leclerc, Int. J. Chem. Kinet. 31 (1999) 361–379.
[16] T. Faravelli, A. Goldaniga, L. Zappella, E. Ranzi, P. Dagaut, M. Cathonnet, Proc. Combust. Inst. 28 (2000) 2601–2608.
[17] J.W. Linnett, W.H. Avery, J. Chem. Phys. 6 (1938) 686–691.
[18] R.S. Rasmussen, R.R. Brattain, J. Chem. Phys. 15 (1947) 120–130.
[19] I.M. Mills, W.L. Smith, J.L. Duncan, J. Mol. Spectrosc. 16 (1965) 349–377.
[20] J.M.R. Stone, J. Mol. Spectrosc. 38 (1971) 503–507.
[21] Y. Koga, S. Kondo, T. Nakanaga, S. Saëki, J. Chem. Phys. 71 (1979) 2404–2411.
[22] S. Kondo, Y. Koga, J. Chem. Phys. 69 (1978) 4022–4031.
[23] A.G. Maki, A.S. Pine, J. Mol. Spectrosc. 112 (1985) 459–481.
[24] G.R. Gladstone, M. Allen, Y.L. Yung, Icarus 119 (1996) 1–52.
[25] R. Prangé, T. Fouchet, R. Courtin, J.E.P. Connerney, J.C. McConnell, Icarus 180 (2006) 379–392.
[26] W.C. Maguire, R.A. Hanel, D.E. Jennings, V.G. Kunde, R.E. Samuelson, Nature 292 (1981) 683–686.
[27] A. Coustenis, R.K. Achterberg, B.J. Conrath, D.E. Jennings, A. Marten, D. Gautier, C.A. Nixon, F.M. Flasar, N.A. Teanby, B. Bézard, R.E. Samuelson, R.C. Carlson, E. Lellouch, G.L. Bjoraker, P.N. Romani, F.W. Taylor, Patrick G.J. Irwin, Thierry Fouchet, A. Hubert, G.S. Orton, V.G. Kunde, S. Vinatier, J. Mondellini, M.M. Abbas, R. Courtin, Icarus 189 (2007) 35–62.
[28] W.F. Wang, J.M. Sirota, D.C. Reuter, J. Mol. Spectrosc. 194 (1999) 256–268.
[29] W.F. Wang, J.M. Sirota, D.C. Reuter, J. Mol. Spectrosc. 198 (1999) 201–208.
[30] F. Hegelund, N. Andresen, J. Mol. Spectrosc. 149 (1991) 305–313.
[31] G. Blanquet, J. Walrand, Spectrochim. Acta Part A: Mol. Spectrosc. 48 (1992) 1231–1233.
[32] J.M. Sirota, D.C. Reuter, J. Frye, J. Quant. Spectrosc. Radiat. Transfer 58 (1997) 145–149.
[33] L. Fissiaux, G. Blanquet, M. Lepère, J. Quant. Spectrosc. Radiat. Transfer 127 (2013) 78–81.
[34] L. Fissiaux, G. Blanquet, J.C. Populaire, M. Lepère, J. Mol. Spectrosc. 296 (2014) 24–27.
[35] R.C. Lord, P. Venkateswarlu, J. Chem. Phys. 20 (1952) 1237–1247.
[36] P.P. Arcas, C. Haeusler, C. MeyerC, N. Van-Thanh, P. Barchewitz, J. Phys. 25 (1964) 667–672.
[37] J. Pliva, C.A. Martin, J. Mol. Spectrosc. 91 (1982) 218–237.
[38] Y. Ohshima, S. Yamamoto, K. Kuchitsu, J. Mol. Spectrosc. 117 (1986) 138–151.
[39] Et. Es-sebbar, Y. Bénilan, A. Farooq, J. Quant. Spectrosc. Radiat. Transfer 115 (2013) 1–12.
[40] Et. Es-sebbar, M. Alrefae, A. Farooq, J. Quant. Spectrosc. Radiat. Transfer 133 (2014) 559–569.
[41] S. Sharpe, T. Johnson, R. Sams, P. Chu, G. Rhoderick, P. Johnson, Appl. Spectrosc. 58 (2004) 1452–1461.
[42] C. Chackerian, S.W. Sharpe, T.A. Blake, J. Quant. Spectrosc. Radiat. Transfer 82 (2003) 429–441.
[43] J.C. Breeze, C.C. Ferriso, C.B. Ludwig, W. Malkmus, J. Chem. Phys. 42 (1965) 402–406.
[44] J.J. Harrison, N.D.C. Allen, P.F. Bernath, J. Quant. Spectrosc. Radiat. Transfer 111 (2010) 357–363.
[45] R.L. Sams, S.W. Sharpe, T.J. Johnson, Presentation in the 60th International Symposium on Molecular Spectroscopy at Columbus, Ohio, US, 2005.
[46] S.J. Yao, J. Overend, Spectrochim. Acta 32 (1976) 1059–1065.
[47] W.F. Wang, A. Stevenson, D.C. Reuter, J.M. Sirota, Spectrochim. Acta Part A 57 (2001) 1603–1610.